



Haptic molecular simulation based on force control

Aude Bolopion, Barthelemy Cagneau, Stephane Redon, Stéphane Régnier

► **To cite this version:**

Aude Bolopion, Barthelemy Cagneau, Stephane Redon, Stéphane Régnier. Haptic molecular simulation based on force control. AIM - 2010 IEEE/ASME International Conference on Advanced Intelligent Mechatronics, Jul 2010, Montréal, Canada. IEEE, pp.329-334, 2010, <10.1109/AIM.2010.5695764>. <hal-00784663>

HAL Id: hal-00784663

<https://hal.inria.fr/hal-00784663>

Submitted on 13 Feb 2013

HAL is a multi-disciplinary open access archive for the deposit and dissemination of scientific research documents, whether they are published or not. The documents may come from teaching and research institutions in France or abroad, or from public or private research centers.

L'archive ouverte pluridisciplinaire **HAL**, est destinée au dépôt et à la diffusion de documents scientifiques de niveau recherche, publiés ou non, émanant des établissements d'enseignement et de recherche français ou étrangers, des laboratoires publics ou privés.

Haptic molecular simulation based on force control

Aude Bolopion, Barthélemy Cagneau, Stephane Redon and Stéphane Régnier

Abstract—In this paper, force control is proposed to connect a molecular simulator to a haptic device. Most of the works dealing with this kind of simulators use position control to manipulate the molecules, with major stability concerns. These two control modes are compared in terms of adequacy with the molecular simulator. Stability with respect to the scaling coefficients introduced to connect the macro and the nanoworlds is also considered. The theoretical results and the experiments carried out confirm that position control is sensitive to the gain tuning. Force control enables to get stable force feedback for varying gains, and is thus a promising coupling to perform manipulations on complex molecular systems.

I. INTRODUCTION

Molecular simulation is one of the fields in which haptic devices greatly improves the user knowledge as well as its ability to perform complex operations, such as prototyping bio-nanorobots [1]. The works can be classified in three main topics: evaluation of the benefits of using haptic, how to interact with large virtual environments using haptic devices, and the choice of the coupling.

The evaluation of haptic for molecular simulators has demonstrated that it helps operators to understand nanoscale phenomena. Its use is recommended for educational purposes [2], [3], but is not limited to academic courses. Chemists and biologists also benefit from haptic to find specific locations in complex molecular systems, such as docking sites [4].

The benefits of haptic feedback depends on the coupling used. In particular, how to reach the entire virtual environment using a haptic device with a limited workspace is a key issue to get an interactive system. Several techniques are proposed, from the concept of clatching (freezing the displacement of the virtual object while enabling the user to modify the position of the haptic handle), to the *Bubble technique* (combination of position and rate control) [5]. As an alternative the concept of *Active Haptic Workspace* is considered [6]. In all cases, when the user is close to the point of interest, a classical position coupling scheme is used to control the object and send the interaction forces to the user. Thus, even if complex techniques are used, the choice of the haptic coupling used when dealing with a precise area of the workspace remains unchanged.

In most of the works dealing with molecular systems

position control is used (the user sets the position of the molecule, and feels the interaction force through the haptic interface). However, stability is difficult to ensure due to long computation times, scaling factors used to link the macro and nano worlds, and the high variation of the forces. Stability is usually guaranteed at the expense of the fidelity of the force feedback. Either the accuracy of the molecular interactions computed is decreased by using simpler models [7], or the damping added to the coupling deteriorates the transparency [8]. This manipulation mode is also not adapted to molecular dynamics simulators, since setting the position of the molecule leads to potentially physically unacceptable positions before shifting to the next step of the simulation, as we will see in this paper. It seems that none of the proposed systems (simulator and haptic coupling) gives satisfying results in terms of the trade off between the accuracy of the computed interaction forces, the stability and the transparency of the force feedback.

In this paper, we present a molecular simulator SAMSON, which enables to simulate complex systems in a few hundreds of milliseconds, and takes into account the flexibility of all the considered molecules. To avoid stability concerns due to the commonly used position control, we propose to use force control. Force control is well known for macro scale teleoperations, but is not used for molecular simulations. The molecular dynamics equation solved by the simulator, on which an additional force can be included, enables to implement this control mode.

Some of the potential applications of our system (conception of new molecules, analysis of molecular properties, ...) are described in [9]. We now present a comparison of position and force control. A detailed description of the molecular simulator and the control schemes, as well as how they are connected, is made to compare the adequacy of the two control modes to molecular dynamics simulators. The stability sensitivity of the coupling schemes, measured as the variation of the magnitude of the roots of the control schemes' transfer functions with respect to given parameters, is considered for the specific application of molecular interactions.

The rest of the paper is organized as follows. In Section II, an overview of the simulator and the coupling is given. Based on the available inputs and outputs, the two control modes (position and force control) are detailed and compared in Sections III and IV in terms of adequacy with the simulator. The stability sensitivity is analyzed in Section V. Experimental results are given in Section VI.

A. Bolopion and S. Régnier are with Institut des Systèmes Intelligents et de Robotique, UPMC - CNRS UMR 7222, 4 Place Jussieu, 75005 Paris, France. {bolopion, regnier}@isir.upmc.fr

B. Cagneau is with Laboratoire d'Ingénierie des Systèmes de Versailles, EA 4048, Université de Versailles Saint Quentin, 45 avenue des Etats Unis, 78035 Versailles, France. barthelemy.cagneau@uvsq.fr

S. Redon is with NANO-D - INRIA Rhône-Alpes, 655 avenue de l'Europe, 38334 Saint-Ismier, France. stephane.redon@inria.fr

II. COUPLING BETWEEN THE HAPTIC INTERFACE AND THE SIMULATION SOFTWARE

A. Molecular simulator SAMSON

SAMSON (System for Adaptive Modeling and Simulation Of Nano-Objects) is based on a quasi-statics method to simulate the motion of the molecular system (Figure 1) [10], [11]. The force field used is derived from a well known molecular mechanics force field, CHARMM [12], which models interactions through van der Waals, electrostatic and dihedral contributions. Our simulator has several specific properties:

- as the simulator solves the equation of motion, the value of the force applied to each atom is directly known (whereas many simulators compute the energy of the system [8])
- both external and internal efforts are computed
- the flexibility of the molecules is simulated, and systems with thousands of degrees of freedom can be handled
- it enables fast computation based on a tree representation of the molecules. The simulation period is only a few hundreds of milliseconds for complex systems.



Fig. 1. Manipulation of a tetraethylammonium (TEA) around a potassium channel (KcsA), 1428 degrees of freedom.

This simulator enables to use two different manipulation modes based on the equation of motion solved for each rigid body. Using spatial notations, this equation is [13]:

$$Ia = F_{ext} + F_{int} - v \times Iv \quad (1)$$

where a (resp. v) is the spatial acceleration (resp. velocity) of the molecule and I is its inertia. F_{ext} are the forces applied by other molecules and F_{int} is the sum of the internal forces.

Considering (1), the user can either manipulate the molecule by setting the position of its center of mass, or by applying a force F_i on it. The first mode is thus the position control in which the *instantaneous position* taken into account while solving (1) is the position that the user sets as the desired position for the molecule. For force control, the user applies an *additional force* to the molecule to be manipulated, so that the equation of motion is modified to:

$$Ia = F_i + F_{ext} + F_{int} - v \times Iv \quad (2)$$

Equations (1) and (2) are integrated with the molecular time T_m . This parameter is introduced since the molecular dynamics do not allow to use the same time basis as the

one we use. A single simulation step (moving the molecule, reconfiguring the system, sending the interaction forces to the user) takes around $T_s = 100\text{ms}$ (simulation loop period), and this corresponds to a period of around $T_m = 2\text{fs}$ for the evolution of the molecular system [14].

The force fed back to the user is F_m :

$$F_m = F_{ext} + F_{int} \quad (3)$$

Thus the user can choose between feeling the internal forces by manipulating a single atom of a molecule, or the total force applied to a given molecule by its environment (while dealing with a whole molecule the internal forces cancel out). Since no modification on our system are necessary the user can easily switch from one mode to the other.

B. Haptic coupling schemes

The quality of the force rendering depends on the control scheme used. The choice of the coupling is thus of utmost importance. When connecting a haptic device to a molecular simulator the delays due to long computations of complex interactions must be taken into account while analyzing the stability. The transfer functions are thus represented using the discrete time variable z . Since the variables coming from the simulator are delayed by one sampling period (period of the simulator), an explicit one step delay is introduced between the simulation and the coupling. This is modeled by the delay operator z^{-1} . The discrete time transfer function $H(z)$ (which input, resp. output, is the force applied to the haptic handle, resp. its position) is computed from the continuous time domain using the Z-transform function [15], and taking into account the effects of the sampler and zero order hold:

$$H(z) = \frac{1}{B_h} \frac{T_s(z - \delta) - (1 - \delta)(z - 1) \frac{M_h}{B_h}}{(z - 1)(z - \delta)} \quad (4)$$

where $\delta = e^{-\frac{B_h T_s}{M_h}}$ and T_s is the simulation's sampling period. M_h and B_h are respectively the master's inertia and viscosity, as given in [16].

Two scaling factors are used to connect the haptic interface and the molecule. The force (resp. position) scaling factor is denoted by A_f (resp. A_d).

Based on the two manipulation modes described above two control schemes with different inputs and outputs can be used, and are described in next sections. Note that, although we have used SAMSON simulator in our implementation, the control schemes we will present may be connected with any simulator which provides access to the required variables (positions, forces, etc.). However, the accuracy of the obtained results (reconfiguration of the molecule, force computed, ...) depend on the accuracy of the simulator.

III. POSITION CONTROL

A. Haptic coupling

The classical impedance display or *Direct Force Feedback (DFB)* coupling, is based on *position control*. It is the simplest structure to connect the haptic device to the simulation

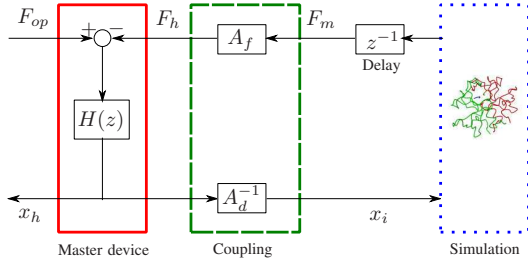


Fig. 2. *DFF* control scheme

using the scaled position of the haptic handle x_i as the input of the molecular dynamics simulator (Figure 2). Only two scaling factors are necessary to control the molecule.

B. Details of the *DFF* algorithm

To compare the adequacy of position and force control with the molecular simulator it is necessary to give some details about how the haptic coupling schemes and the simulation are connected. This is done in this section for the *DFF* coupling, and in Section IV-B for force control. Figure 3 gives more details about the notations used.

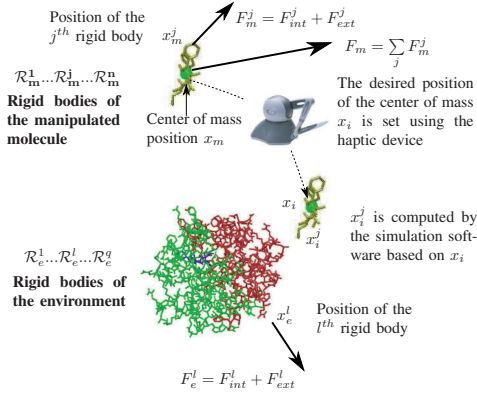


Fig. 3. Notations and principle of position control

As mentioned in [9], the calculations of positions and forces performed by the simulation software are made on each rigid body. However, for ease of manipulation, the user manipulates the molecule as a whole, controlling the position of the center of mass x_i . As explained in Section II, the instantaneous position of the molecule considered when solving the equation of motion (1) is the desired position of the rigid body. Internal and external forces are computed and used to update the positions of the molecules in the environment and their *internal* degrees of freedom (to simulate their flexibility). This reconfiguration step involves a modification of the rigid bodies positions, and thus the actual position of the center of mass of the manipulated molecule x_m might be different from the one set by the user using the haptic interface x_i (see Algorithm 1¹).

¹For the sake of clarity only the translations are considered in this algorithm. Rotations are implemented using the same methodology. This remark is also valid for Algorithm 2.

Algorithm 1 Position control algorithm

- 1) Compute the desired position of the center of mass $x_i(k+1)$ set by the operator using the control scheme (position of the haptic handle scaled by A_d).
- 2) Set the position of the rigid bodies to $x_i^j(k+1)$, computed as the relative positions with respect to x_i .
- 3) Update all interatomic forces $F_m^1(k+1), \dots, F_m^n(k+1)$ (resp. $F_e^1(k+1), \dots, F_e^q(k+1)$) applied to the rigid bodies which are inside (resp. outside) the manipulated molecule using the molecular simulator.
- 4) Compute the sum $F_m(k+1) = \sum_{j=1}^n F_m^j(k+1)$ of the forces applied to the molecule, and send it to the user.
- 5) Update the positions x_m^j (resp. x_e^l) of the rigid bodies which are inside (resp. outside) the manipulated molecule using the quasi-statics simulator. Note that in the following equations $x_i^j(k+1)$ (resp. $F_m^j(k+1)$ and $F_e^l(k+1)$) are known since they have previously been computed: Step 2 (resp. 3) of the algorithm.

$$x_m^j(k+1) = x_i^j(k+1) + \frac{T_m^2}{m_j} F_m^j(k+1)$$

$$x_e^l(k+1) = x_e^l(k) + \frac{T_m^2}{m_l} F_e^l(k+1)$$

The *DFF* coupling has one main drawback: the position the user sets using the haptic interface might be physically unacceptable (i.e., with high potential energy due to atomic clashes). Even if the next step of the simulation corrects the position, this can lead to instabilities, and the forces sent to the user may misrepresent the correct molecular interactions.

IV. FORCE CONTROL

A. Haptic coupling

In the *Force-Force (FF)* coupling scheme (Figure 4), the input of the simulation is the force applied by the user to the molecule. In addition to the scaling factors A_f and A_d

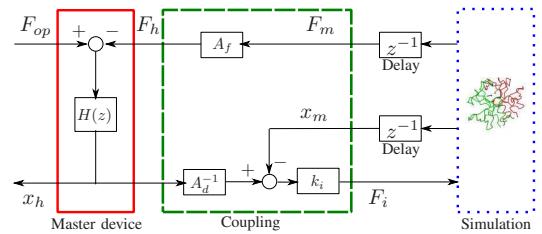


Fig. 4. *FF* control scheme

already considered on the *DFF* coupling, a proportional gain k_i is introduced. This gain adjusts the magnitude of the force applied to molecule, which is based on the difference between the molecule and the haptic handle positions.

B. Details of the *FF* algorithm

Contrary to the *DFF* algorithm, the simulator's input is the force F_i that the user wants to apply to the entire molecule.

This force is set by controlling the distance between the haptic handle and the molecule positions. The corresponding forces applied on each rigid body F_i^j of the manipulated molecule as well as the environment forces are used to update the position of all the rigid bodies (inside and outside the manipulated molecule) using (2) (see Algorithm 2).

Algorithm 2 Force control algorithm

- 1) Compute the force applied by the operator to the molecule using the control scheme: $F_i(k+1) = k_i \left[\frac{x_h(k+1)}{A_d} - x_m(k) \right]$
- 2) Compute the force $F_i^j(k+1) = F_i(k+1)/n$, applied to all the j^{th} rigid bodies of the manipulated molecule.
- 3) Update the positions x_m^j (resp. x_e^l) of the rigid bodies which are inside (resp. outside) the manipulated molecule using the quasi-statics simulator. Note that in the following equations, $F_i^j(k+1)$ is known since it has previously been computed in Step 2:

$$x_m^j(k+1) = x_m^j(k) + \frac{T_m^2}{m_j} (F_m^j(k) + F_i^j(k+1))$$

$$x_e^l(k+1) = x_e^l(k) + \frac{T_m^2}{m_l} F_e^l(k)$$

- 4) Update all interatomic forces $F_m^1(k+1), \dots, F_m^n(k+1)$ (resp. $F_e^1(k+1), \dots, F_e^q(k+1)$) applied to the rigid bodies which are inside (resp. outside) the manipulated molecule using the molecular simulator.
 - 5) Compute the sum $F_m(k+1) = \sum_{j=1}^n F_m^j(k+1)$ of the forces applied to the molecule, and send it to the operator.
-

Using force control enables to integrate the user's input while solving the mechanical equation (2). Contrary to the *DFE* manipulation mode, the position of the molecule is always physically acceptable, which avoids instabilities due to atomic clashes. Thus, this manipulation mode is more adapted to the molecular simulator than position control.

V. COMPARISON OF THE CONTROL SCHEMES STABILITY

In this section, the sensitivity of the coupling schemes' stability is compared. Since passivity is conservative (it ensures stability for any operator and any environment as long as they are themselves passive) [17], it is not used in this work. To compare the haptic coupling schemes, the action of the operator is not taken into account, and a simplified model of the environment is considered (an equivalent spring constant k_e). This is obviously not enough to model the complex interactions between molecules, but comparisons on the control schemes' stability can be made. The sensitivity analyzed is the variation of the magnitude of the roots of the transfer functions' characteristic equations with respect to given parameters. We choose to analyze here the influence of the scaling factors.

A. Characteristic equations

The discrete time transfer function of the *DFE* control scheme is derived from the coupling presented in Figure 2:

$$Z \left\{ \frac{x_h(s)}{F_{op}(s)} \right\} = \frac{X_h(z)}{F_{op}(z)} \quad (5)$$

$$= \frac{T_s \frac{z-\delta}{z-1} - (1-\delta) \frac{M_h}{B_h}}{B_h(z-\delta) + \left[T_s \frac{z-\delta}{z-1} - (1-\delta) \frac{M_h}{B_h} \right] \frac{A_f}{A_d} k_e z^{-1}} \quad (6)$$

where Z is the Z-transform function, and δ is the parameter defined in (4). The corresponding characteristic equation is:

$$a_3 z^3 + a_2 z^2 + a_1 z + a_0 = 0 \quad (7)$$

where:

$$a_3 = B_h, \quad a_2 = -B_h(1+\delta)$$

$$a_1 = \delta B_h + \left(T_s - (1-\delta) \frac{M_h}{B_h} \right) \frac{A_f}{A_d} k_e$$

$$a_0 = \left(-\delta T_s + (1-\delta) \frac{M_h}{B_h} \right) \frac{A_f}{A_d} k_e$$

The transfer function of the *FE* coupling is computed according to Figure 4:

$$\frac{X_h(z)}{F_{op}(z)} = \frac{H(z)}{1 + H(z)G(z) \frac{A_f}{A_d}} \quad (8)$$

where: $G(z) = \frac{F_m(z)}{X_h(z)} = \frac{k_i k_e T_m^2}{mz(z-1) + k_i T_m^2 + k_e T_m^2}$ and m is the total mass of the molecule. The characteristic equation is:

$$b_4 z^4 + b_3 z^3 + b_2 z^2 + b_1 z + b_0 = 0 \quad (9)$$

where:

$$b_4 = mB_h, \quad b_3 = -(2+\delta)mB_h$$

$$b_2 = (k_i + k_e)T_m^2 B_h + mB_h(1+2\delta)$$

$$b_1 = -(1+\delta)(k_i + k_e)T_m^2 B_h - \delta mB_h$$

$$+ \left[T_s - (1-\delta) \frac{M_h}{B_h} \right] k_i k_e T_m^2 \frac{A_f}{A_d}$$

$$b_0 = B_h \delta (k_i + k_e) T_m^2$$

$$+ \left[-T_s \delta + (1-\delta) \frac{M_h}{B_h} \right] k_i k_e T_m^2 \frac{A_f}{A_d}$$

Analytical stability criteria can be obtained for both of these control schemes using the Jury criterion [15], as it is done in [18] for a control scheme similar to the *DFE* one. However, the relations derived are complex and the influence of the control scheme parameters on stability is not highlighted. Thus, in the next section a numerical analysis is performed.

B. Numerical comparison of stability

For both the *DFE* and *FE* control schemes two parameters can be tuned to ensure stability: the force and the displacement scaling factors. The force scaling factor A_f is chosen so that the user can distinctly feel the interaction forces between and/or within the molecules. Thus, only the displacement coefficient can be modified. A numerical analysis of the influence of A_d on each control scheme is performed: the variations of the highest magnitude of the roots (absolute number of the largest pole) of the characteristic equations (7) and (9) are considered in Figure 5. The numerical values used correspond to the experiments carried out in the following

sections. They are given in Paragraph VI-A. Different values of the environment stiffness have been considered, from $k_e = 1\text{N.m}^{-1}$ to $k_e = 1000\text{N.m}^{-1}$.

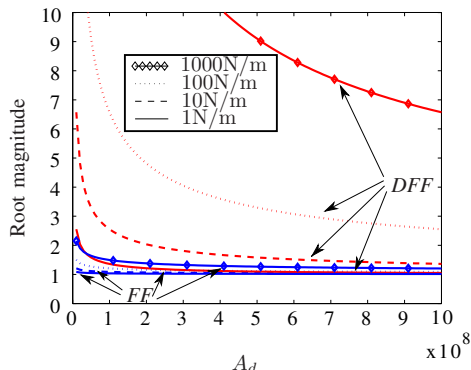


Fig. 5. Variations of the magnitude of the roots against A_d , for different environment stiffness k_e . For clarity, only the highest magnitude is plotted for each control scheme given the stiffness.

The variations of the magnitude of the roots are of particular interest. For both of the control schemes, small values of A_d and/or stiff environments may lead to an unstable system. The magnitude of the roots of the *DFF* control scheme quickly increases when A_d is decreased, or k_e is increased. On the contrary, the roots obtained with the *FF* control scheme are almost constant. Thus, the *DFF* control scheme stability is more sensitive than the *FF* one to the variations of A_d for a given environment stiffness k_e . This result is confirmed experimentally in the next section.

VI. EXPERIMENTAL COMPARISON OF THE CONTROL SCHEMES

An experiment involving a classical blocker of potassium channels (KcsA), the tetraethylammonium (TEA) is performed. The docking of the TEA into KcsA is studied in particular in the context of mutagenesis studies to determine the influence of aromatic residues on the external blockade of the TEA. The experiment consists in approaching the *TEA* from the potassium channel and then moving it away. The complexity of this example (5 molecules involved, for a total of 1428 degrees of freedom) is representative of the molecular systems biologists and chemists consider. This experiment performed for both the *DFF* and *FF* control schemes for varying values of A_d is presented to support the conclusions of Section V-B. More examples can be found in [9].

A. Characteristic parameters

The parameters of this experiment are: $m = 1.8 \cdot 10^{-25}\text{kg}$ (mass of the *TEA* : the molar mass is 110g/mol in the CHARMM19 representation in which the 20 hydrogen atoms are not represented), $T_s = 138 \cdot 10^{-3}\text{s}$ (simulation period, as it varies depending on the number of atoms involved in molecular interactions, the largest one is given), $T_m = 2 \cdot 10^{-15}\text{s}$ (physical integration period), $d = 8\text{\AA}$ (cutoff distance used to limit the computational time due to the molecular interactions that can be felt at infinite distance),

$A_f = 0.3 \cdot 10^9$ (force amplification), $k_i = 24\text{N.m}^{-1}$ (for the *FF* coupling). The 124 *dof* the most important for the accuracy of the molecular interaction computation are activated by our adaptive simulator [10]. The position scaling factor depends on the user needs (precise or fast manipulation). To test the sensitivity of the control schemes' stability with respect to this parameter, three experiments are performed, with $A_d = 0.50 \cdot 10^9$ (*Experiment A*), $A_d = 0.25 \cdot 10^9$ (*Experiment B*) and $A_d = 0.125 \cdot 10^9$ (*Experiment C*). The haptic interface used is a Phantom Omni device from Sensable (Figure 1), with an inertia $M_h = 0.072\text{kg}$ and a viscosity $B_h = 0.005\text{N.s.m}^{-1}$ [16].

B. Experimental results

For each experiment, the tetraethylammonium is approached and retracted from the potassium channel. The movement is directed along one axis. The forces returned to the operator are depicted in Figures 6, 7 and 8².

For both of the coupling schemes, the user distinctly feels the interaction forces since they are rendered with a force in the order of the newton. As predicted in Section V-B, as A_d

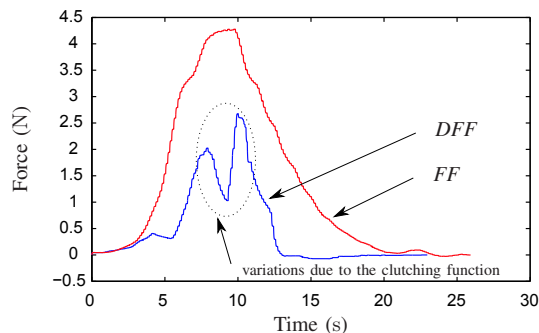


Fig. 6. Haptic force during *Experiment A* (124 activated *dof*)

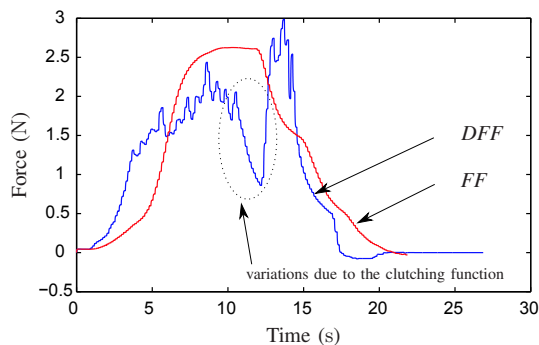


Fig. 7. Haptic force during *Experiment B* (124 activated *dof*)

is decreased, the *DFF* control scheme becomes unstable. In experiment C, atom clashes produce high magnitude forces and instabilities. On the contrary, the *FF* coupling scheme remains stable. The maximum force varies depending on the exact displacement performed by the user. The variations on the force profile of the *DFF* control scheme (see circles in Figures 6 and 7) are due to the manipulation mode. As

²To avoid damages on the haptic interface forces are limited to 3N

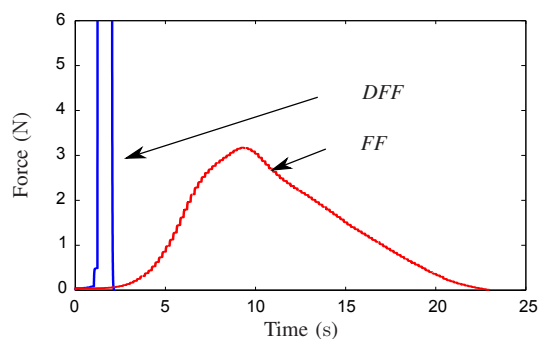


Fig. 8. Haptic force during *Experiment C* (124 activated dof)

the user freezes the movement of the molecule to reach a more comfortable position with the haptic interface the rest of the system applies forces to the molecules, which moves according to (1). This is not the case for the *FF* control scheme since the user does not apply a force on the molecule even while clutching its position.

Both the conclusions of Sections III-B and IV-B, the numerical comparison of stability (Section V-B), and the experiments highlight that force control is well suited for molecular manipulation and enables a stable coupling. More experiments were made on different molecules (HIV virus, water molecules, ...), and similar conclusions were observed. The results are not displayed here since they do not provide additional information. More examples can be found in [9].

Adding damping to the *DFF* coupling would improve the stability, but transparency would be deteriorated. Since molecular interactions involve complex variations of the forces and efforts of small magnitude (in particular for attractive interactions), transparency is a major concern to provide to the user a high fidelity force feedback. It can be noted that for both the *DFF* and *FF* control schemes the user feels the interaction forces scaled by the force coefficient. Thus, high fidelity force feedback is ensured.

VII. CONCLUSION

Position control, which is commonly used to connect a haptic device to a molecular simulator has two major drawbacks: due to the equation of motion solved, the position set by the user can be physically unacceptable before being updated, which can produce instabilities. The second drawback is that the stability of the control scheme is very sensitive to the scaling factors used, which can limit its potential applications. On the contrary, force control offers both a good adequacy with the simulation software and the stability is not sensitive to the chosen gain parameters. Since the molecular simulator used is able to simulate the flexibility of complex molecules composed of thousands of degrees of freedom, our system improves the user's understanding of molecular interactions.

Besides the two criterion used in this paper to compare the control schemes, the user feeling should also be taken into account, as well as the intuitiveness of the manipulation mode. User based tests should thus be carried out in future

works to perform a detailed comparison. Solutions to automatically determine the most appropriated scaling factors and gains for the control schemes should also be considered. Adaptive gains might be a solution to improve the *DFF* control scheme performances.

VIII. ACKNOWLEDGMENT

This work was supported by the French National Agency of Research, through the *PACMAN* project.

REFERENCES

- [1] M. Hamdi, A. Ferreira, G. Sharma, and C. Mavroidis, "Prototyping bio-nanorobots using molecular dynamics simulation and virtual reality," *Microelectronics Journal*, vol. 39, no. 2, pp. 190–201, 2008.
- [2] P. Persson, M. Cooper, L. Tibell, S. Ainsworth, A. Ynnerman, and B.-H. Jonsson, "Designing and evaluating a haptic system for biomolecular education," in *IEEE Virtual Reality Conference*, 2007, pp. 171–178.
- [3] J. Murayama, H. Shimizu, C. S. Nam, H. Satoh, and M. Sato, "An educational environment for chemical contents with haptic interaction," in *Proceedings of the International Conference on Cyberworlds*, 2007, pp. 346–352.
- [4] F. P. Brooks, Jr., M. Ouh-Young, J. J. Batter, and P. Jerome Kilpatrick, "Project GROPE - Haptic displays for scientific visualization," in *Proceedings of the 17th annual conference on Computer graphics and interactive techniques*, 1990, pp. 177–185.
- [5] L. Dominjon, A. Lécuyer, J.-M. Burkhardt, G. Andrade-Barroso, and S. Richir, "The "Bubble" technique: interacting with large virtual environments using haptic devices with limited workspace," in *Proceedings of the First Joint Eurohaptics Conference and Symposium on Haptic Interfaces for Virtual Environment and Teleoperator Systems*, 2005, pp. 639–640.
- [6] E. Subasi and C. Basdogan, "A new haptic interaction and visualization approach for rigid molecular docking in virtual environments," *Presence: Teleoperators and Virtual Environments*, vol. 17, no. 1, pp. 73–90, 2008.
- [7] Y.-G. Lee and K. W. Lyons, "Smoothing haptic interaction using molecular force calculations," *Computer-Aided Design*, vol. 1, pp. 75–90, 2004.
- [8] B. Daunay and S. Régnier, "Stable six degrees of freedom haptic feedback for flexible ligand-protein docking," *Computer Aided Design*, vol. 41, no. 12, pp. 886–895, 2009.
- [9] A. Bolopion, B. Cagneau, S. Redon, and S. Régnier, "Haptic feedback for molecular simulation," in *Proceedings of the IEEE International Conference on Intelligent Robots and Systems*, 2009, pp. 237–242.
- [10] R. Rossi, M. Isorce, S. Morin, J. Flocard, K. Arumugam, S. Crouzy, M. Vivaudou, and S. Redon, "Adaptive torsion-angle quasi-statics: a general simulation method with applications to protein structure analysis and design," *Bioinformatics*, vol. 23, no. 13, pp. i408–417, 2007.
- [11] S. Grudinin and S. Redon, "Practical modeling of molecular systems with symmetries," *Journal of Computational Chemistry*, 2010, to appear.
- [12] B. Brooks, R. Bruccoleri, D. Olafson, D. States, S. Swaminathan, and M. Karplus, "CHARMM: A program for macromolecular energy, minimization, and dynamics calculations," *Journal of Computational Chemistry*, vol. 4, pp. 187–217, 1983.
- [13] R. Featherstone, *Robot dynamics algorithms*. Kluwer Academic Publishers, 1987.
- [14] J. E. Stone, J. Gullingsrud, and K. Schulten, "A system for interactive molecular dynamics simulation," in *Proceedings of the symposium on Interactive 3D graphics*, 2001, pp. 191–194.
- [15] K. Ogata, *Discrete-time control systems - second edition*. Prentice-Hall, 1995, ch. 3-4, pp. 83–90/182–192.
- [16] N. Diolaiti, G. Niemeyer, F. Barbagli, and J. Salisbury, "Stability of haptic rendering: Discretization, quantization, time delay, and coulomb effects," *IEEE Transactions on Robotics*, vol. 22, no. 2, pp. 256–268, 2006.
- [17] H. K. Khalil, *Nonlinear systems*, 3rd ed., P. Education, Ed. Prentice Hall, 2002.
- [18] J. J. Gil, E. Sánchez, T. Hulin, C. Preusche, and G. Hirzinger, "Stability boundary for haptic rendering: Influence of damping and delay," *Journal of Computing and Information Science in Engineering*, vol. 9, no. 1, p. 011005, 2009.